Journal of Research on the Lepidoptera 35:61–77, 1996 (2000)

Flexural stiffness patterns of butterfly wings (Papilionoidea)

Scott J. Steppan

Committee on Evolutionary Biology, University of Chicago, Chicago, IL 60637, USA., E-mail: *steppan@bio.fsu.edu*

Abstract. A flying insect generates aerodynamic forces through the active manipulation of the wing and the "passive" properties of deformability and wing shape. To investigate these "passive" properties, the flexural stiffness of dried forewings belonging to 10 butterfly species was compared to the butterflies' gross morphological parameters to determine allometric relationships. The results show that flexural stiffness scales with wing loading to nearly the fourth power ($p_w^{3.9}$) and is highly correlated with wing area cubed ($S^{3.1}$).

The generalized map of flexural stiffness along the wing span for *Vanessa cardui* has a reduction in stiffness near the distal tip and a large reduction near the base. The distal regions of the wings are stiffer against forces applied to the ventral side, while the basal region is much stiffer against forces applied dorsally. The null hypothesis of structural isometry as the explanation for flexural stiffness scaling is rejected. Instead, selection for a consistent dynamic wing geometry (angular deflection) in flight may be a major factor controlling general wing stiffness and deformability. Possible relationships to aerodynamic and flight habit factors are discussed. This study proposes a new approach to addressing the mechanics of insect flight and these preliminary results need to be tested using fresh wings and more thorough sampling.

Key Words: biomechanics, butterfly wings, flight, allometry, flexural stiffness, aerodynamics

Introduction

A flying insect generates aerodynamic forces primarily through the active manipulation of wing movements and the "passive" morphological properties of deformability and wing shape. The morphological parameters of insect flight have been the subject of various investigations (Weis-Fogh 1977, Wootton 1981, Ellington 1984, Betts 1986, Dudley 1990, Srygley 1994), complimenting an extensive body of work on the aerodynamics of insect and hovering flight (e.g., Jensen 1956, Weis-Fogh 1973, Nachtigall 1974, Ellington 1980, 1984b). However, empirical measures of aerodynamically relevant mechanical properties of wings are absent from the literature.

Present address: Department of Biological Science, Florida State University, Tallahassee, FL 32306-1100

Paper submitted 24 September 1997; revised manuscript accepted 8 May 1998.

Various measures of wing geometry have been used as surrogates for the biomechanical properties of wings, but these can be only crude approximations given the complex structure and construction of wings. Here, I measure the deformability of butterfly wings to determine its interspecific scaling relationships with various wing and body size parameters. This investigation complements qualitative analyses of structure and allometry, theoretical predictions of wing properties, and observations of flight performance and behavior.

Previous studies of insect flight have investigated the aerodynamics of flight through theoretical calculations (Weis-Fogh 1977, Ellington 1980), allometric patterns of wing shape and wing beat (Greenewalt 1962, Ellington 1984), wing movements and deformations during flight (Wootton 1981, Betts 1986), flight habit and behavior (Betts & Wootton 1988, Dudley 1990, Srygley 1994), the aerodynamic effects of angle of attack or presence of scales (Jensen 1956, Nachtigall 1974, Martin & Carpenter 1977), and common structural features of butterfly wings (Wootton 1981). To date, no study has measured deformability of wings. This study will demonstrate the potential of biomechanical approaches to understanding insect flight.

Flexural stiffness (*EI*) is a measure of deformability, which by controlling wing shape under aerodynamic load modifies aerodynamic forces. The flexural stiffness of a structure is a function of two properties: the elastic modulus (*E*, stress per unit strain) of the material that composes it; and the second moment of inertia (*I*), a function of the cross-sectional geometry. This study will 1) determine flexural stiffness patterns within butterfly wings, and 2) define allometric relationships among flexural stiffness and morphological parameters. Analysis of allometric patterns can provide insights into the importance of developmental or structural constraints relative to presumptive adaptations (Strauss 1990).

Some expectations for flexural stiffness patterns can be drawn from previous studies. Betts (1986) found that in a small sample of Heteroptera, angular deformation of the wing tip was weakly correlated with angular momentum of the wing. A principal conclusion derived from Betts (1986) and Wootton (1981) is that dorsal transverse flexion (producing a dorsally concave surface) is more strongly resisted by wing structure (i.e., ventrally stiffer) than is ventral transverse flexion. Wootton hypothesized that ventral flexion may reduce drag on the upstroke of wings exhibiting minimal wing-twisting, as in Lepidoptera. These studies would predict 1) that stiffness will decrease in the distal region, possibly associated with a flexion line (see Wootton, 1981 for detailed explanation), and 2) ventral stiffness (e.g., resistance to ventrally directed forces which would produce dorsal transverse flexion) will be significantly greater than dorsal stiffness.

Two alternative hypotheses regarding interspecific scaling of flexural stiffness are tested. H_0: the measured index of flexural stiffness is entirely a mechanical consequence of structural and geometric isometry. H_1: the index of flexural stiffness scales so that angular deflection under proportionate loading regimes remains consistent (cf. elastic similarity; McMahon,

1973). The predictions based on these hypotheses are presented in the Discussion.

Materials and Methods

Species selected and morphometric measures

Three individuals for each of ten species were included among a mixed dry butterfly set obtained from Carolina Biologic Supply Company. The 10 species were *Battus polydamas* Linnaeus 1758 (Papilionidae) *Parides montezuma* Westwood 1842 (Papilionidae), *Danaus lotis* Cramer 1779 (Nymphalidae), *Phoebis statira* Cramer 1777 (Pieridae), *Eurema hecabe* Linnaeus 1758 (Pieridae), *Pereute charops* Boisduval 1836 (Pieridae), *Ascia monuste* Linnaeus 1758 (Pieridae), *Pyrrhogyra neaerea* Linnaeus 1758 (Nymphalidae), the heliconiine *Dione juno* Cramer 1782 (Nymphalidae), and the pierid *Catopsillia scylla* Linnaeus 1764. Two living *Vanessa cardui* Linnaeus 1758 (Nymphalidae) were included, and their wings measured both immediately after death and after three weeks of desiccation. Species were identified according to Lewis (1974). For each specimen, total body mass and mass of the right fore- and hindwing separately, were weighed with a Mettler H80 electro-balance (0.1 mg precision). Fore- and hindwings were drawn to scale using a camera lucida attached to a Wild microscope at magnification x6. These outlines were then digitized to determine wing area.

Flexural stiffness measures

The principal set of measurements consisted of force/deformation curves from forewings under cantilever loading to produce transverse bending (Fig. 1). These curves were generated for all 11 species. Cantilever loading was chosen over alternatives such as three- and four-point bending because, in natural flight, the base of the wing is fixed relative to the body while the remainder of the wing is aerodynamically loaded along its length as nearly perpendicular to the plane of the wing as possible. The 10 dried species were compared for allometric patterns in wing area (S), wing loading (dry body mass/wing area; r_w), and flexural stiffness (EI) as a function of dry body mass (m). Calculated wing loading will underestimate actual wing loading because dried specimens were used. All wings were loaded both dorsally and ventrally. As described in this paper, loading from the dorsal direction (dorsal loading) results in a dorsally convex surface, which is equivalent to ventral transverse flexion in other studies.

Two *Vanessa cardui* adults were tested two to three days after emergence from chrysalides. They were killed by pinching their thorax and then placed in a freezer for five minutes, immediately after which they were weighed. After the *V. cardui* were loaded in the tensiometer, they were allowed to dry for two to three weeks, then weighed and loaded again to provide an estimate of the effects that drying had produced upon the properties of the wings. A detailed map was made of stiffness along the span of a single *Vanessa cardui* wing. Use of dried wings hinders accurate estimation of flexural stiffness under natural conditions. For allometric studies though, the effects of drying need only be consistent across taxa. If drying does vary in its effects along the wing, this could bias interpretation of the wing maps

Basal attachment regions of individual forewings were glued using cyanoacrylate

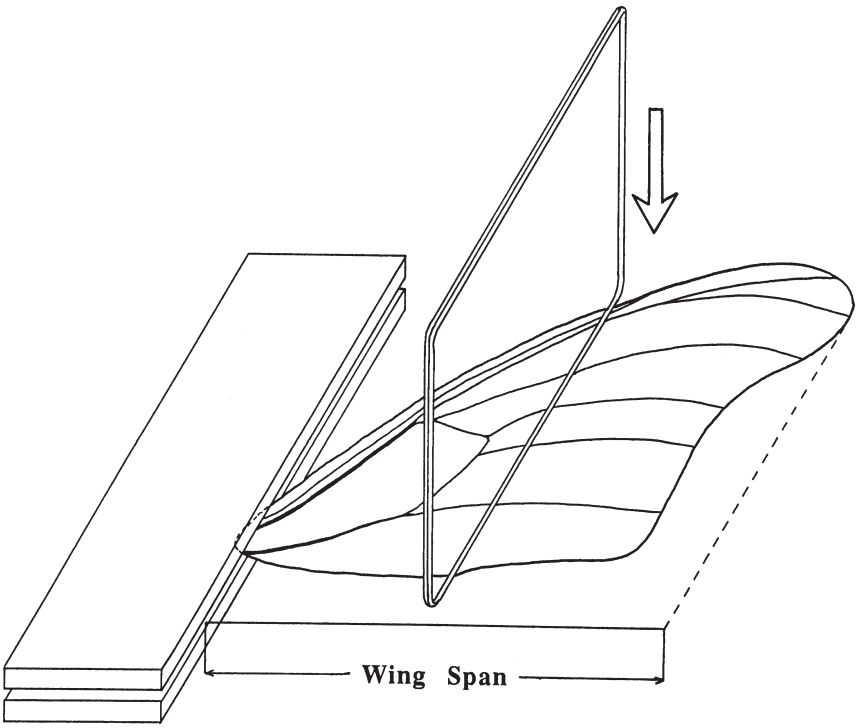

Figure 1. Diagrammatic representation of the method by which the wings were loaded for the stiffness measures. The rectilinear loading bar was displaced horizontally into the wing as indicated by the arrow. Measurements were taken at specified distances perpendicular to the line between wing base and tip. Remainder of the tensiometer apparatus not shown.

between two glass microscope slides. Spacers were placed between the glass slides to prevent crushing of the wing. Only one to two millimeters were grasped in this way, allowing the remainder of the wing to flex freely. Any discrepancy in the estimate of the actual place of attachment will affect stiffness calculations near the base much more than near the tip, because flexural stiffness varies with "beam" length to the third power. For example, an underestimate of 0.4 mm at 10% of wing length in the finely sampled *Vanessa cardui* (27 mm total length) would underestimate stiffness by 30%, while the same error at 90% of wing length would only underestimate stiffness by 5%. Wings were positioned with the span oriented perpendicular to the loading bar (Fig. 1).

The other principal wing deformations of camber and torsion are very important in wing aerodynamics, but are more difficult to measure accurately. Transverse flexion is observed widely in lepidopteran wings (Wootton 1981) and is amenable to experimental control. The loading bar was positioned using a millimeter scale at predetermined distances from the secured wing base (20%, 40%, 60%, and 80% of wing span) perpendicular to wing span. Another measurement was made at ap-

proximately 0.5 mm less than 100% wing span because loading at 100% wing span would result in the bar slipping off the wing. The wings were loaded in cantilever bending by fixing the glass slide grips to the carriage of a tensiometer. The loading bar, whose position could be adjusted with an accuracy estimated at ±0.4 mm, was displaced horizontally into the wing from either the dorsal or ventral directions. The diameter of the loading bar used in most measurements (including the detailed mapping) was 1.0 mm. Some of the wings wore loaded with a 2.5 mm diameter bar.

Fore wings were loaded in a tensiometer designed and assembled by M. LaBarbera. Displacement of the wing at the loading bar was measured by an LVDT, linear variable differential transformer (7307, Pickering, New York, USA), with a linear range of 2.5 mm attached to the carriage of the tensiometer. Force was measured by a force transducer (FTD-6-l0 10 g, Schaevitz, New Jersey, USA), accurate to $\pm 7 \times 10^{-6}$ N at the most sensitive setting. The LVDT was calibrated by inserting the core rod a distance measured using an attached scale (±0.05 mm). The force transducer was calibrated by hanging known weights from the transducer when aligned vertically. Force and displacement were recorded on a chart recorder (2200, Gould, Ohio, USA). In regions of linear response of force to displacement, the slope was used to estimate the force (F) and displacement (D). These variables were then used to calculate flexural stiffness by the formula:

$$EI = (F * L^3 / (3 * D) \quad (1)$$

where EI is flexural stiffness in N m^2, F is force in Newtons, D is displacement at the loading bar in meters, and L is the length of the wing segment under bending (Wainwright et al. 1982) . This formula applies to a cantilever beam of uniform EI. The region between 60% and 80% of the wing span showed relatively constant stiffness. An index of flexural stiffness, *EI(W),* was derived for each wing by averaging the dorsal and ventral stiffnesses at 60% and 80% wing spans. Averaging these four measures also reduced the expected error in EI that were due to errors in positioning the loading bar.

It must be emphasized that each position's EI is calculated assuming uniform material properties throughout the section under load. Therefore, the maps of EI do not plot *local* stiffness, but rather the integral of stiffness of the wing up to that position. Although this should not significantly affect the overall pattern, dorsal versus ventral differences basally could obscure discrimination of differences distally. For example, ventral stiffness in the tip region may actually be greater than that calculated for mean *El*, but deflections for a given load may be similar because of greater deformation in the basal region under ventral loading.

Allometric patterns were determined by regressing morphological parameters and the index of flexural stiffness. Species means were used rather than individual measurements to avoid inflating the degrees of freedom in statistical tests, because within species values are naturally correlated due to phylogenetic relatedness. Reduced major axes (RMA) were calculated rather than least squares regressions because RMA is more appropriate for allometric investigation (Rayner 1985).

Degree of distastefullness for each species to avian predators was provided by R.

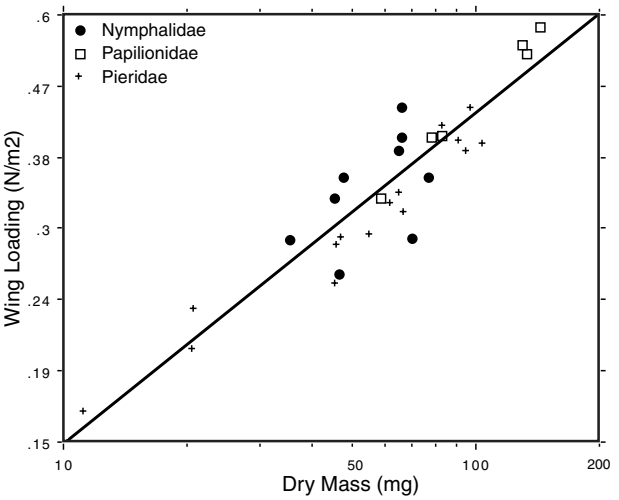

Figure 2. Log wing loading versus log dry body mass for 30 individuals representing 10 species. The RMA equation for the log-transformed data is l_{pw}=0.516 mm$^{-0.811}$ (r^2=0.810).

Srygley (Chai 1986, 1988).

Results

Morphometric scaling

The slope of a regression line on a log-log plot defines the exponent in a power function relationship of the form $y=ax^b$. Log-transformed measures of wing area (S) were regressed against log-transformed total mass for the 10 dry species means. Isometric scaling would produce a regression line with slope of 2/3 ($S=am^{2/3}$). The reduced major axis (RMA) slope obtained for the 10 dry species means, 0.582, is not significantly less than 2/3 (r^2=0.846). Wing loading shows weak positive allometry; wing loading scales with the square root of mass (RMA=0.516, r^2=0.81), almost significantly different (P=0.06) from the null hypothesis of isometric scaling ($m^{1/3}$) (all 30 individuals shown in Figure 2). Additionally, wing area scaled isometrically with dry wing mass ($m_w^{0.70}$, n=10), therefore, wings are not becoming proportionately thicker (ignoring wing architecture like pleating). No strong conclusions regarding any taxonomic pattern can be drawn, given the small sample size, although nymphalids appear to have relatively higher wing loadings than pierids.

Flexural stiffness maps

The effect of drying on wing stiffness was estimated by measuring two *Vanessa cardui* wings immediately after killing the butterflies and then again after two to three weeks of drying. Drying appears to significantly increase stiffness, but the overall pattern of stiffness across the wing remains roughly

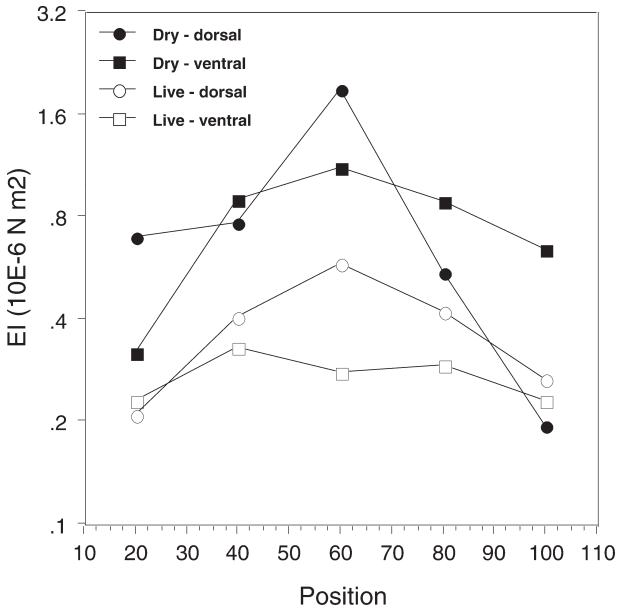

Figure 3. Effect of drying on wing stiffness averaged for the two *Vanessa cardui*. *EI* (10^{-6} kg m^2) plotted on log scale. *EI* values represent stiffness of entire wing up to measurement point.

similar with peak stiffness in the middle region (Fig. 3). Differences do exist between the patterns in the two conditions, primarily in the distal and proximal measurements (e.g., low dorsal stiffness at the tip for dry wings), and these may be due small errors in positioning the bar. Stiffness decreases rapidly in the distal 1.0 mm, and positioning errors are magnified in the basal region because of the cubic relationship between length and stiffness. Flexural stiffness (*EI*) for 10 species was determined for five positions along the wing both dorsally and ventrally. *EI* values ranged over two orders of magnitude from 2.3×10^{-8} N m^2 to 1.49×10^{-6} N m^2 (Table 1). Because wings varied so greatly in stiffness, values were normalized by dividing each wing's set of measurements by the maximum stiffness measured for that wing. The 10 wing maps so derived could then be compared as a proportion of maximum stiffness for each wing position. The normalized stiffness maps are displayed in Figure 4a. A single factor ANOVA showed that for the pooled data set (dorsal plus ventral), all adjacent positions (e.g. 40% with 20% and 60%) were significantly different in *EI* except for the 60% and 80% pair. The relative constancy in this region is one of the reasons that *EI* at 60% and 80% were averaged to give *EI*(*W*). An average wing is clearly stiffer under dorsal loading along the basal 40% of wing span. More pronounced than at 40%, the dorsally loaded wing is 55% stiffer at 20% of wing span ($P<0.001$). The distal 40% is less stiff under dorsal loading than ventral loading, but the difference is less pronounced and not statistically significant.

Table 1. Mean morphometric and flexural stiffness measures for the 10 species of butterflies acquired as dry specimens; wing loading in mg cm^2, flexural stiffness measures (*EI*) in 10^{-6} Kg m^2. Upper row for each species represent dorsal measures, lower row the ventral measures. Blank entries represent missing data for stiffness measures or not applicable to dorsal/ventral distinction. (p) = palatable, (u) = unpalatable, (–) = palatability unknown.

Direction	Species	dry mass (mg)	wing area (cm^2)	wing loading (N/m^2)	*EI*(20)	*EI*(40)	*EI*(60)	*EI*(80)	*EI*(100)	*EI*(*W*)
dorsal	*Parides montezuma* (u)	78.1	19.02	0.400	0.534	0.633	0.934	0.543	0.209	0.894
ventral	(Papilionidae)				0.373	0.422	1.367	0.734	0.333	
dorsal	*Battus polydamus* (u)	143.6	24.49	0.574	1.149	1.486	1.037	0.939	0.568	1.106
ventral	(Papilionidae)				0.428	0.672	1.226	1.220	0.375	
dorsal	*Pyrrhogyra neaerea* (p)	65.0	16.50	0.386	0.172	0.422	0.249	0.142	0.081	0.217
ventral	(Nymphalidae)				0.083	0.199	0.272	0.204	0.285	
dorsal	*Danaus lotis* (u)	70.2	23.74	0.290	0.715	0.971	0.758	0.528	0.227	0.716
ventral	(Nymphalidae)				0.304	1.002	0.896	0.683	0.240	
dorsal	*Dione juno* (u)	35.4	12.03	0.288	0.037	0.059	0.081	0.073		0.088
ventral	(Nymphalidae)				0.023	0.053	0.094	0.105		
dorsal	*Catopsilla scylla* (–)	45.7	17.96	0.250	0.276	0.324	0.461	0.299	0.154	0.431
ventral	(Pieridae)				0.211	0.379	0.474	0.450	0.198	
dorsal	*Eurema hecabe* (p)	20.8	8.86	0.230	0.053	0.062	0.044	0.074		0.063
ventral	(Pieridae)				0.044	0.071	0.074	0.062		
dorsal	*Phoebis statira* (p)	91.2	22.50	0.397	0.450	0.640	0.745	0.763	0.523	0.744
ventral	(Pieridae)				0.286	0.466	0.721	0.746	0.543	
dorsal	*Pereute charops* (–)	97.7	21.72	0.441	1.041	1.170	0.990	0.855	0.414	0.802
ventral	(Pieridae)				0.396	0.729	0.722	0.640	0.435	
dorsal	*Ascia monuste* (u)	55.3	18.52	0.294	0.129	0.438	0.461	0.393	0.201	0.416
ventral	(Pieridae)				0.250	0.318	0.502	0.309	0.309	

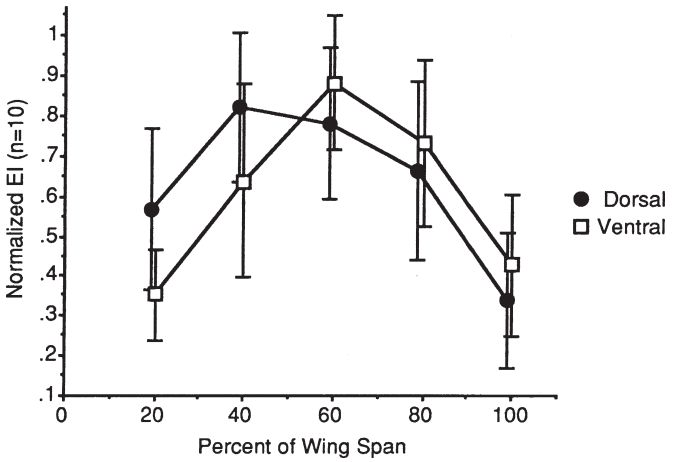

Figure 4a. Map of normalized stiffnesses for the mean values for 10 butterfly species under dorsal and ventral loading. Original measurements were normalized as a proportion of the maximum stiffness measured for each wing. Standard deviation bars shown. All positions are significantly different from each other except 60% and 80% ($P<0.05$) . *EI* values represent stiffness of entire wing up to measurement point.

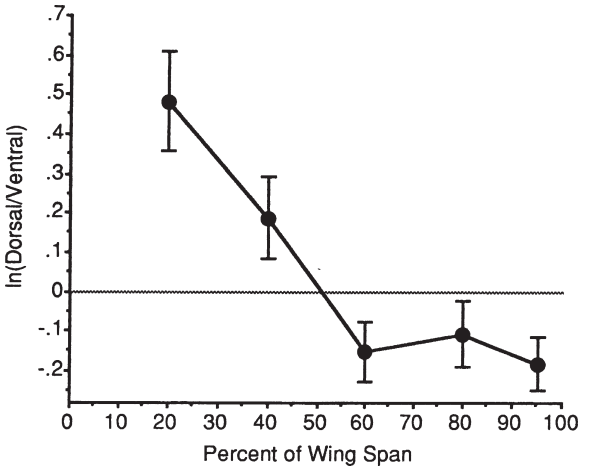

Figure 4b. Mean ratios of dorsal versus ventral stiffnesses by wing position. Standard error bars shown. Only at 20% of wing span are dorsal and ventral differences significantly different ($P<0.001$).

The 60% position shows a significant difference only at the 90% confidence level while the 40%, 80%, and 100% positions do not show significant differences (P>0.2). The relative stiffnesses of dorsal versus ventral are summarized in Figure 4b.

Figure 4a illustrates a possible common pattern across species but is a rather crude map of dorsal and ventral flexural stiffness along wing span. It also blends together slightly different stiffness patterns among species. To complement this data set, a dried forewing of *V. cardui* was mapped with much finer resolution, at approximately 1.4 mm intervals (Figure 5a). The general pattern is in agreement with the averaged wing map. The wing is dorsally stiffer (i.e., against ventral flexion) in the basal 60%, particularly in the basal 40%. The distal 20% to 30% seems to be slightly stiffer ventrally. When *EI* is plotted on a log-scale, two features stand out (Figure 5b). First, stiffness from 40% to 85% of wing span is relatively constant compared to the rest of the wing. Second, within the basal 25%, the wing is dorsally much stiffer than ventrally; on average about three times stiffer. The accuracy of *EI* estimates is lowest very near the base (e.g. <3 mm), due to small errors in distance measures from the actual base of the wing.

Flexural stiffness and morphological parameters

The index of flexural stiffness, *EI*(*W*), was regressed against several common wing parameters, using mean values for each species. It was hypothesized that by structural necessity, *EI*(*W*) would be correlated with wing loading, and indeed, *EI(W)* scales with wing loading to nearly the fourth power (3.9) with a moderate correlation coefficient of 0.598. Longer, more heavily loaded wings would need to be stiffer to prevent excessive deformation. However, *EI*(*W*) is more strongly correlated with dry body mass (r^2=0.814, RMA slope=1.80). The correlation of *EI(W)* with relative wing thickness (total dry wing mass/total wing area) drops to 0.417 (RMA slope=0.928). The strongest correlation is with wing area; r^2=0.911 (Figure 6). *EI(W)* scales with wing area cubed ($S^{3.1}$; 90% confidence interval, 2.46-3.73).

Figure 6 is slightly curvilinear. The power function provides a much better fit to the data than a simple linear model (r^2=0.785) which predicts zero stiffness at l0 cm^2. The remaining apparent curvilinearity is likely taxon specific. The two nymphalid species are approximately 40% less stiff than predicted by the regression, whereas the smaller of the papilionids is 64% stiffer than predicted. These would result in deflections 60% more or less than expected respectively.

The residuals from a polynomial regression constrained to pass through the origin were compared for two groups: those palatable to birds and unpalatable. The mean residuals were not significantly different between the two groups (P>0.5), indicating that palatable butterflies do not have relatively stiff wings.

Discussion

Various selective forces and phylogenetic constraints have been proposed to account for insect wing morphology. The functional constraint of ther-

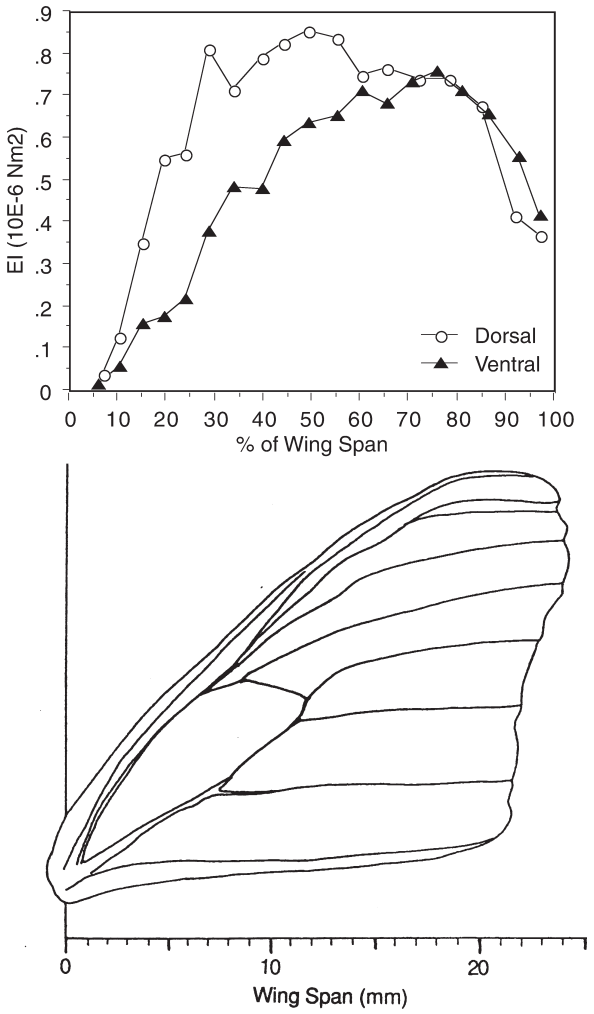

Figure 5a. Wing stiffness map for a dry *Vanessa cardui* individual. Below is a diagram of the wing, drawn to the same scale as the X-axis of the stiffness map. The loading bar was oriented parallel to the Y-axis. *EI* values represent stiffness of entire wing up to measurement point.

moregulation may well have been significant during the early evolution of insect wings (Kingsolver and Koehl 1985). However, thermoregulation is probably of little importance to major scaling and structural patterns in butterflies because only the proximal 15% of the wing surface plays a significant role in conductive heat transfer to the body (Wasserthal 1975) and the combination of pigmentation and behavior significantly effect thermoregulation in species that utilize the entire wing (Kingsolver 1985). Strauss' (1990) study of shape allometry in nymphalids suggests that aerodynamic (i.e., functional) constraints may be less important than sexual (i.e.,

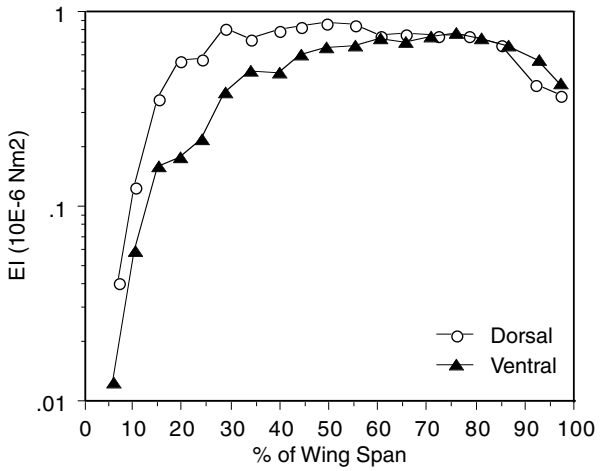

Figure 5b. Log-scaled wing stiffness map for a dry *Vanessa cardui* individual, illustrating the relatively constant stiffness from 40% to 85% of wing span and the large differences between dorsal and ventral stiffness basally.

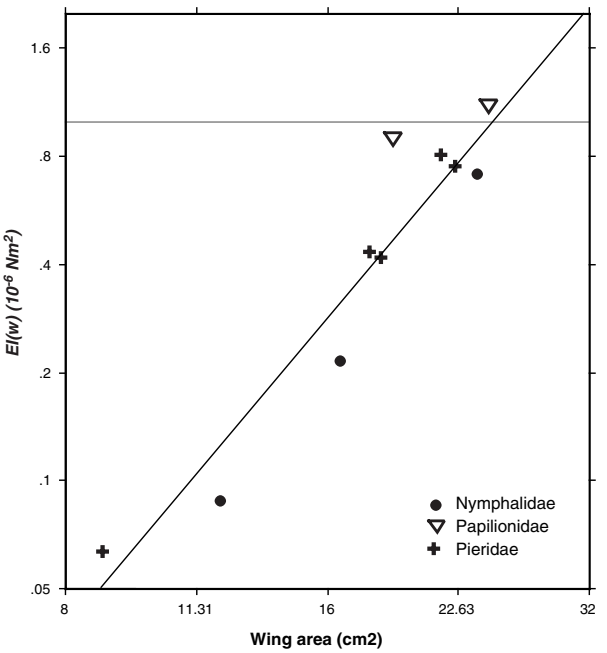

Figure 6 . Index of flexural stiffness, *EI(W)*, versus wing area, *S*. Log-log scale. RMA equation is $\ln EI(W) = 3.1S - 9.78$ ($r^2 = 0.911$).

display related) selection. Butterflies have unusually large wings used to attract mates, to confuse or warn predators, for camouflage, and for other display-related functions.

Scaling

The wing and body morphology measured in this study do not scale isometrically among the butterfly species sampled. Although wing thickness seems to scale isometrically, wing area shows a slight negative allometry with dry body mass. As a consequence, wing loading shows positive allometry. In addition, $EI(W)$ increases more rapidly than any of the other parameters, and is most highly correlated with wing area. These results do not indicate strong selection for an optimal wing loading that is size-independent.

The impact of allometrically induced variation in propulsion related forces has been examined in other organisms. Because flying squirrel patagium did not scale so as to minimize allometric variation in wing loading, Thorington and Heaney (1980) concluded that other selective factors must be involved, resulting in size related differences in gliding habit and maneuverability. In response to isometric scaling, changes in the geometric alignment and utilization of propulsive limbs in mammals can compensate for size-dependent increases in mechanical stresses (Biewener 1989). These compensations can significantly limit maneuverability and accelerative ability. Possible examples of compensation in butterflies include flight habit and wing-stroke frequency. Indeed, Betts and Wootton (1988) found tendencies in flight mode among a small sample of butterflies to be associated with size and shape parameters of wings, including wing loading.

The results in this study can be compared to those reported elsewhere (Greenewalt 1962, Kokshaysky 1977, Dudley 1990). Greenewalt's analysis is generally in accord with the wing area/body mass result, but in disagreement with wing thickness. Greenewalt found that wing area increased with the 0.60 power of wing mass, and thus wing thickness increased with the 1.34 power of wing span. The result from this study is almost significantly different from Greenewalt's figure ($P<0.10$). It should be noted at this point that reanalyses of the original data (Magnan 1934, Sotavalta 1947) show a slightly weaker relationship but a similar slope than he reported ($r^2=0.702$ versus 0.772; RMA=0.652 versus his mean regression line 0.634). The reanalysis standardized sample sizes at one individual per species (n=20). As Kokshaysky (1977) also noted, the number of data points graphed (35) exceeded those listed in the regression table (33) and the number with complete data (23).

Two hypotheses of flexural stiffness allometry were tested; structural isometry and consistent dynamic wing geometry. For a beam with rectangular cross-section, I, the second moment of area, is a product of width*thickness^3. Assuming isometry, width and thickness will be proportional to L, yielding by substitution, $I \propto L^4$. Area is proportional to L^2, and thus, EI should scale with area S^2. The hypothesis that EI scales isometrically with wing area is rejected because the allometric coefficient of 3.1 is significantly different from 2.0 ($P<0.02$).

Alternatively, aerodynamic constraints could result in angular deflection remaining constant; i.e., *EI* compensates for scaling in mass and wing area so as to maintain a size independent dynamic wing geometry. This concept is congruent with the elastic similarity which McMahon (1973, 1975) developed and applied to a variety of issues including tree shape and quadraped locomotion. Deformation may be the most important structurally controlled property of lepidopteran wings affecting aerodynamics. Greenewalt (1975) argued that if wing thickness scales isometrically, angular deflection should remain constant (since his results did not indicate isometry, he concluded that angular deflection must show negative correlation with size). However, under the assumption that deflection of the wing scales isometrically (D/L=constant c), rearrangement of eq. 1 yields a prediction for *EI*.

$$EI = F*L^2/3c \qquad (2)$$

If, instead of inputting the experimental force that was used to calculate *EI,* we assume that the principal forces acting on the wing are proportional to body weight, and replace *EI* with *EI*(*W*), then eq. 2 predicts that *EI* is proportional to weight x wing area (L^2, assuming on average, wing shape scales isometrically). Multiplying wing loading by the area yields the total force acting on the wing; total body weight. (In addition, the virtual mass of the accelerated air can range from 0.3 [Diptera] to 1.3 [Odonata] times the wing mass [Ellington, 1984]. Virtual mass has not been taken into account in this analysis.) The results are close to the prediction; *EI* scales with $(m*S)^{1.16}$ (r^2=0.882). The hypothesis of constant angular deflection cannot be rejected.

Wing stiffness patterns

The reduction in distal stiffness matches the expectation of previous workers. In Heteroptera, significant reduction in inertial stresses may be achieved by lightening the fore wing distally (Betts 1986), thereby reducing stiffness. Betts views transverse [ventral] flexion as improving aerodynamics by "optimizing camber and angle of attack ..., minimizing adverse aerodynamic forces at stroke reversal, ... creating favourable unsteady forces at stroke reversal" (1986, p. 298). Wootton (1981) felt that ventral flexion would preferentially reduce drag on the upstroke. The hypothesis of a structural basis for the limited dorsal flexion seen in previous studies is not strongly supported by the results of this study. The differences in the magnitude of *EI* appear to be less than the difference between dorsal and ventral deflections described by Betts and Wootton. Distal deflection will be affected by loading distribution in addition to structural properties. Differences in distal load may be due to differences in angular velocity, or related to the effects of angle of attack stemming from camber and torsion elsewhere on the wing. For example, *Pieris brassicae* supinates its wings on the upstroke to an angle of attack near zero, thus significantly reducing the force generated during the upstroke (Ellington 1980).

Perhaps the most striking result of the present work is the very low stiffness near the wing base. The thickening of the veins and wing structure observed near the base would be expected to increase the second moment of area, *I*, and therefore flexural stiffness. Although the smaller chord width near the base will reduce *I*, this reduction in width alone would seem insufficient to account for the magnitude of change documented here given that thickness increases near the base would increase stiffness. Some functional advantages may be suggested. Low ventral stiffness basally may permit wing geometries that facilitate the "clap and fling" mechanism for generating lift (see Weis-Fogh [1973] for description). This stiffness pattern would seem to be disadvantageous during normal flapping flight, where a stiff wing would transmit muscle power to the surrounding air more efficiently. If greater ventral flexibility is found to be aerodynamically disadvantageous, then these results imply that the requirements for initial take off using clap and fling impose the greater functional constraints and stronger selective forces on wing design.

Alternatively, the low stiffness at the base relative to the center of wing span may act to increase wing accelerations at stroke reversal in much the same manner as a whip. This flexibility may also reduce inertial stress, especially at stroke reversal. Basal curvature appears greatest near stroke reversal in high speed photos of butterflies in flight (Dalton 1975). These possibilities need to be tested further as well as testing whether the biomechanical properties of the glue and apparatus used to grasp the wing base account for some of the reduced stiffness measured near the wing base.

No association was found between relative stiffness and palatability to avian predators. A relationship might be expected if palatable species must be stronger fliers to escape predators (Srygley 1994) and if stronger fliers have stiffer wings. The findings here can be compared with those of Srygley (1994) who found that palatability was most strongly associated with positions of centers of body and wing mass, which related to flight speed and turning performance, but was less strongly associated with measures of wing shape.

At present, improved understanding of the phylogenetic and ecological contexts of butterfly flight are most needed in order to synthesize the biomechanical and performance studies. There appears to be a strong phylogenetic component to relative wing stiffness, with the nymphalids having relatively flexible wings and the papilionids having stiff wings. Future studies with greater taxonomic sampling should incorporate explicitly the phylogenetic relationships in order to avoid inflating significance levels, using, for example, independent contrasts rather than raw species values in the regression (Felsenstein 1985). Particularly important is the need to incorporate flight performance and flight habit parameters in studies such as Betts and Wootton (1988) and Dudley (1990), along with structural biomechanics and ecological correlates on comparable species.

The results of this study should be viewed as preliminary and subjected to further testing and refinement. Fresh rather than dried wings must be

measured to avoid the assumptions of proportional effects of drying, both among species and across wings. Applying the load to the wing along a chord of constant rotational radius may be preferable to the transverse orientation used here. Local rather than integrated stiffnesses should be measured. The wing orientation chosen by Betts and Wootton (1988; fig. 2), which is rotated approximately 20° posteriorly relative to this study, may be more representative of loadings experienced during natural flight. The orientation used in this study is sometimes observed at stroke reversal (Betts & Wootton 1988). Furthermore, neither camber nor torsion were examined, and deformations and wing movements usually involve all three. However, this study introduces an approach based on direct measurement of the biomechanical properties of wings that has heretofore not been addressed. Biomechanical studies are currently the missing link between studies of allometry, flight performance, ecology, wing geometry, and theoretical aerodynamics.

Acknowledgements. Sincere thanks must go to M. LaBarbera for his generous contributions of time, expertise, encouragement, and for the use of his experimental equipment. R. Srygley generously provided the information on palatability. M. Morgan, R. Srygley, K. Roy, R. Robbins, W. Watt, and four anonymous reviewers provided suggestions that significantly improved the content of this manuscript.

Literuature Cited

Betts, C.R. 1986. Functioning of the wings and axillary sclerites of Heteroptera during flight. Journal of Zoology, London (B) 1:283–301.

Betts, C.R., & R.J. Wootton. 1988. Wing shape and flight behavior in butterflies (Lepidoptera: Papilionoidae and Hesperioidae): a preliminary analysis. Journal of Experimental Biology 138:271–288.

Biewener, A.A. 1989. Scaling body support in mammals: limb posture and muscle mechanics. Science 245:45–48.

Chai, P. 1986. Field observations and feeding experiments on the responses of rufous-tailed jacamars (*Galbula ruficauda*) to free-flying butterflies in a tropical rainforest. Biological Journal of the Linnean Society 29:161–189.

Chai, P. 1988. Wing coloration of free-flying Neotropical butterflies as a signal learned by a specialized avian predator. Biotropica 20:20–30.

Dalton, S. 1975. Borne on the Wind. Reader's Digest Press, New York.

Dudley, R. 1990. Biomechanics of flight in neotropical butterflies: morphometrics and kinematics. Journal of Experimental Biology 150:37–53.

Ellington, C.P. 1980. Vortices and hovering flight. Pp. 64-101. in W. Nachtigall (ed.), Instationäre Effekte an schwingeden Tierflügeln. Mainze: Akademie der wiss u. d. Literatur, Weisbaden. Franz Steiner Verlag GMBH, Weisbaden.

Ellington, C.P. 1984. The aerodynamics of hovering insect flight. II. Morphological parameters. Philosophical Transactions of the Royal Society, London (B) 305:17–40.

Felsenstein, J. 1985. Phylogenies and the comparative method. American Naturalist 125:1–15.

Greenewalt, C.H. 1962. Dimensional relationships for flying animals. Smithsonian Miscellaneous Collections 144:1–46.

Greenewalt, C.H. 1975. The flight of birds. Transactions of the American Philosophical Society 65:1–67.

Jensen, M. 1956. Biology and physics of locust flight. III. The aerodynamics of locust flight. Philosophical Transactions of the Royal Society, London (B) 239:511–552.

Kingsolver, J.G. 1985. Thermoregulatory significance of wing melanization in *Pieris* butterflies (Lepidoptera: Pieridae): physics, posture, and pattern. Oecologia 66:546–553.

Kingsolver, J.G., & M.A.R. Koehl. 1985. Aerodynamics, thermoregulation, and the evolution of insect wings: differential scaling and evolutionary change. Evolution 39:488–504.

Kokshaysky, N.V. 1977. Some scale dependent problems in aerial animal locomotion. Pp. 421–436. in T.J. Pedley (ed.), Scaling Effects in Animal Locomotion. Academic Press, London.

Lewis, H.L. 1974. Butterflies of the World. Harrap, London.

Magnan, A. 1934. Le vol des insectes. Herman et Cie, Paris.

Martin, C.J., & P.W. Carpenter. 1977. Flow-visualization experiments on butterflies in simulated gliding flight. Fortschritte der Zoologie 24:307–316.

McMahon, T. 1973. Size and shape in biology. Science 179:1201–1204.

——. 1975. Using body size to understand the structural design of animals: quadrapedal locomotion. Journal of Applied Physiology 39:619–627.

Nachtigall, W. 1974. Insects in Flight. McGraw-Hill, New York.

Rayner, J.M.V. 1985. Linear relations in biomechanics: the statistics of scaling functions. Journal of Zoology, London (A) 206:415–439.

Sotavalta, O. 1947. The flight tone (wing-stroke frequency) of insects. Acta Entomologica Fennica 4:1–117.

Srygley, R.B. 1994. Locomotor mimicry in butterflies? The associations of positions of centres of mass among groups of mimetic, unprofitable prey. Philosophical Transactions of the Royal Society, London (B) 343:145–155.

Strauss, R.E. 1990. Patterns of quantitative variation in lepidopteran wing morphology: the convergent groups Heliconiinae and Ithomiinae (Papilionoidae: Nymphalidae). Evolution 44:86–103.

Thorington, R.W., & L.R. Heaney. 1980. Body proportions and gliding adaptations of flying squirrels (Petauristinae). Journal of Mammalogy 69:101–114.

Wainwright, S.A., W.D. Biggs, J.D. Currey, & J.M. Gosline. 1982. Mechanical Design in Organisms. Princeton University Press, Princeton.

Wasserthal, L.T. 1975. The role of butterfly wings in regulation of body temperature. Journal of Insect Physiology 21:1921–1930.

Weis-Fogh, T. 1973. Quick estimates of flight fitness in hovering animals, including novel mechanisms for lift production. Journal of Experimental Biology 59:169–230.

——. 1977. Dimensional analysis of hovering flight. Pp. 405–420 in T.J. Pedley (ed.), Scaling Effects in Animal Locomotion. Academic Press, London.

Wootton, R.J. 1981. Support and deformability in insect wings. Journal of Zoology, London 193:447–468.